TIME DOMAIN CHARACTERISTICS OF BROADBAND ANTIPODAL FERMI ANTENNA AND ITS APPLICATION TO THROUGH-WALL IMAGING

Hiroyasu SATO, Yukiko TAKAGI,
Yoshihiko WAGATSUMA†, Koji MIZUNO† and Kunio SAWAYA
Graduate School of Engineering, Tohoku University
Aza-Aoba 05, Aramaki, Aobaku, Sendai, 980-8579, Japan
† Research Institute of Electrical Communication, Tohoku University
2-1-1, Katahira, Aobaku, Sendai, 980-8577, Japan
E-mail: sahiro@ecei.tohoku.ac.jp

1. INTRODUCTION

There is a great demand for broadband antennas used for many applications such as the ultra-wideband (UWB) communications, the EMI measurements and the wideband radars. Considering the transmission and reception of pulse signals, not only broadband characteristics of input impedance and radiation pattern but also the distortionless condition are required. Among many types of broadband antennas such as the bow-tie antenna, the log-periodic dipole array antenna, the spiral antenna, the TEM horn antenna and the double ridged horn antenna, the tapered slot antenna (TSA) is well known as traveling wave operation, low weight, thin structure, easy to fabricate, well suited for microwave integrated circuits (MICs) and is expected for the applications described above.

Recently, Sugawara et al. have proposed a TSA called "Fermi antenna" [1] having a profile defined by the Fermi-Dirac function as well as the corrugation on the side of the substrate. In our previous paper [2], the antipodal Fermi antenna (APFA) with the combination of antipodal feeding section [3] and Fermi-Dirac taper section has been proposed and high gain and the lower cross polarization level are obtained in a broadband frequency range. The FDTD analysis was also performed showing that the VSWR and the radiation patterns were almost agree with the measured data.

In this paper, time domain characteristics of the APFA designed in [2] are investigated. 2-element H-plane APFA array is also developed as a quasi-monostatic pulse radar for the application of through-wall imaging.

2. GEOMETRY

Fig. 1 shows the geometry of the APFA. The Fermi-Dirac taper is determined by $f(x) = a/(1+e^{-b(x-c)})$ [4]-[6] where a denotes the asymptotic value of the width of the taper for $x \to \infty$ and c denotes the x coordinate of the inflection point of the Fermi-Dirac function. Because of the relation of $f'(c) = ab/4$, b is related to the gradient at the inflection point c. Also there is a relation of $f(c) = a/2$ and $W = 2a$ when $b(L-c) \gg 1$. Dimensions of the APFA are shown in Fig. 1.

3. EXPERIMENTS

The vector network analyzer 8722ET (Agilent Technologies) is used for frequency-domain measurement. The time-domain data were obtained by the frequency-domain data in the frequency range from 2GHz to 18GHz (Bandwidth=16GHz) which yield a time resolution of Δt=0.0625ns.

The transmission coefficient S_{21} between two APFAs separated with a distance d in the opposite direction was measured. Fig. 2 shows the magnitude of S_{21} and the group delay as a function of frequency. Almost constant magnitude and group delay are observed in the frequency range above 7.5GHz. The limit of the lower frequency is caused by the length of the corrugation l_c because the corrugation works when $l_c \geq 0.1\lambda$ [2]. Fig. 3 shows the pulse response. Quite

ISBN: 89-86522-78-0 94460©KEES

small distortion of the time response is observed. The time delay of each peak of magnitude is $\tau\,(d{=}0){=}1.97\,\mathrm{ns}$, $\tau\,(d{=}0.5\,\mathrm{m}){=}3.65\,\mathrm{ns}$, $\tau\,(d{=}1\,\mathrm{m}){=}5.33\,\mathrm{ns}$, for $d{=}0$, 0.5 m and 1 m, respectively, and relation $c\,(\tau\,(0.5\,\mathrm{m}){-}\tau\,(0)) = c\,(\tau\,(1\,\mathrm{m}){-}\tau\,(0.5\,\mathrm{m})) = 504\,\mathrm{mm}$ is obtained.

In order to apply the APFA to a quasi-monostatic pulse radar shown in Fig. 4, mutual coupling between two APFAs was measured. Fig. 5 shows the magnitude of the mutual coupling between two parallel APFA elements as a function of frequency. It is observed that the mutual coupling is quite small in the frequency range above 7GHz and is less than -20dB for above 4.2GHz in the case of $D_H{=}37\,\mathrm{mm}$.

Fig. 6 shows the measured pulse response when a metal plate is located in front of the APFAs with distances $d{=}0.5\,\mathrm{m}$, 0.8 m. Peaks of magnitude at $t{=}2.05\,\mathrm{ns}$ are observed for both cases as well as the case without the metal plate which corresponds to the direct coupling. Peaks of magnitude are $t\,(d{=}0.5\,\mathrm{m}){=}5.33\,\mathrm{ns}$ and $t\,(d{=}0.8\,\mathrm{m}){=}7.39\,\mathrm{ns}$ for $d{=}0.5\,\mathrm{m}$ and 0.8 m, respectively. The estimated distance using $\tau\,(0){=}1.97\,\mathrm{ns}$ are $c\,(t\,(0.5\,\mathrm{m}){-}\tau\,(0)) = 504\,\mathrm{mm}$ and $c\,(t\,(0.8\,\mathrm{m}){-}\tau\,(0)) = 813\,\mathrm{mm}$ and almost the same to the real distances.

A through-wall imaging was performed by the 2-dimensional scanning of 2-element H-plane APFA array. Fig. 8 shows the experimental setup, where a metal ruler supported by a metal cylinder, a wood cylinder are located behind a plywood wall with metal frame. The scanning area of $1\,\mathrm{m}{\times}1\,\mathrm{m}$ on $y{=}0$ plane are indicated in Fig. 8. Fig. 9 shows the pulse response at $P_1\,(x{=}330\,\mathrm{mm},\ y{=}0,\ z{=}630\,\mathrm{mm})$, $P_2\,(x{=}330\,\mathrm{mm},\ y{=}0,\ z{=}520\,\mathrm{mm})$ and $P_3\,(x{=}330\,\mathrm{mm},\ y{=}0,\ z{=}200\,\mathrm{mm})$. The reflected wave from the plywood wall is observed at $t{=}3.3\,\mathrm{ns}$ and peaks of magnitude at $t{=}3.29\,\mathrm{ns}$ (P_1), $5.16\,\mathrm{ns}$ (P_2) and $7.53\,\mathrm{ns}$ (P_3) are corresponding to the reflected wave from the metal frame of plywood wall, the metal ruler and the wood cylinder, respectively.

Magnitude of time response at $t{=}3.29\,\mathrm{ns}$, $5.16\,\mathrm{ns}$ and $7.53\,\mathrm{ns}$ on the scanning area is shown in Fig. 10. The images corresponding to the delay time of reflected waves from three objects are obtained. The image of the width of metal ruler is almost 200mm which is 5 times greater than the real width of 40mm. The 3dB beam width in both the E-plane and the H-plane of the APFA at 10GHz is 36 degrees and the low angular resolution causes the low spatial resolution of images [2].

4. CONCLUSION

Time domain characteristics of the APFA were investigated experimentally. It was found that the distortionless condition is almost satisfied in the broadband frequency range. A quasi-monostatic pulse radar was developed using 2-element H-plane APFA array and applied to through-wall imaging.

ACKNOWLEDGEMENT

This work was partially supported by Information Synergy Center, Tohoku University.

REFERENCES

[1] S. Sugawara, Y. Maita, K. Adachi, K. Mori and K. Mizuno, "A mm-wave tapered slot antenna with improved radiation pattern," IEEE MTT-S International Microwave Symposium Digest, pp. 959–962, Denver, USA, 1997.

[2] Y. Takagi, H. Sato, Y. Wagatsuma, K. Sawaya and K. Mizuno, "Study of high gain and broadband antipodal Fermi antenna with corrugation," International Symposium on Antennas and Propagation, vol. 1, pp. 69-72, Sendai, Japan, 2004.

[3] E. Gazit, "Improved design of the Vivaldi antenna," IEE proc. H, Vol. 135, No. 2, pp. 89-92, 1988.

[4] H. Sato, N. Arai, Y. Wagatsuma, K. Sawaya and K. Mizuno, "Design of Millimeter Wave Fermi Antenna with Corrugation," IEICE Trans. (B), vol. J86-B, no. 9, pp. 1851–1859, 2003 (in Japanese).

[5] H. Sato, K. Sawaya, N. Arai, Y. Wagatsuma and K. Mizuno, "Broadband FDTD Analysis of Fermi Antenna with Narrow Width Substrate," IEEE Antennas and Propagation Society International Symposium, vol. 1, pp. 261-264,Ohio, USA, 2003.

[6] H. Sato, S. Kagaya, Y. Wagatsuma, K. Sawaya and K. Mizuno, "Design of Narrow-width Fermi Antenna with Circular Radiation Pattern," International Symposium on Antennas and Propagation, vol. 2, pp. 765-768, Sendai, Japan, 2004.

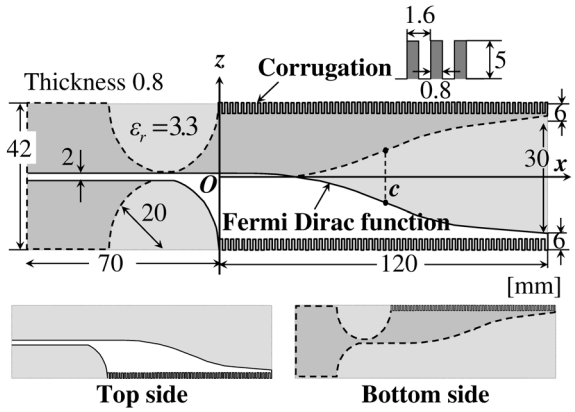

Figure 1: Geometry of APFA.

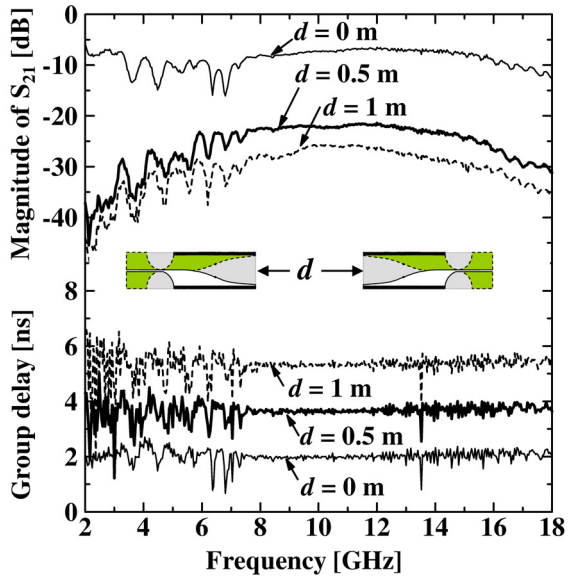

Figure 2: Magnitude of S_{21} and group delay of two APFAs as a function of frequency.

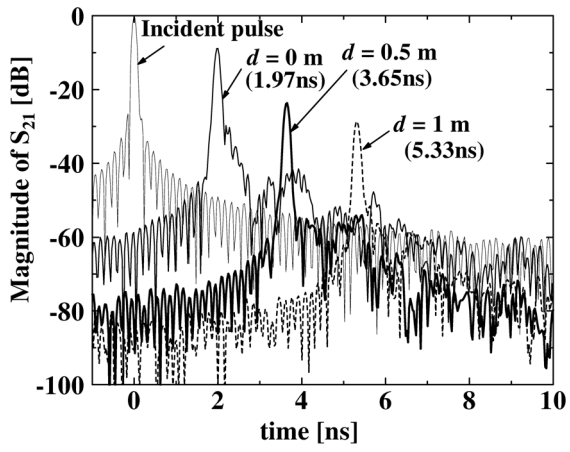

Figure 3: Pulse response of two APFAs.

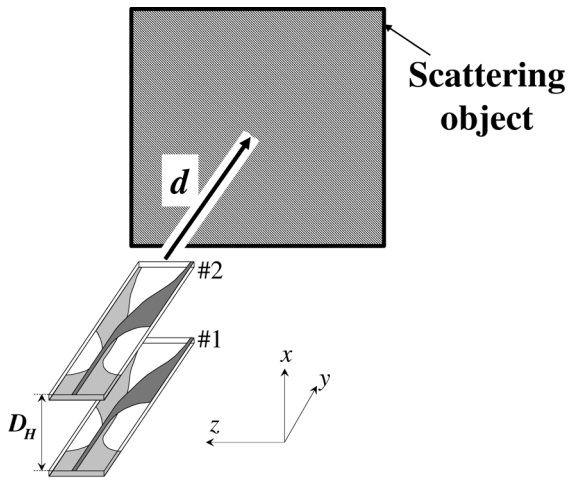

Figure 4: 2-element H-plane APFA elements for quasi-monostatic pulse radar.

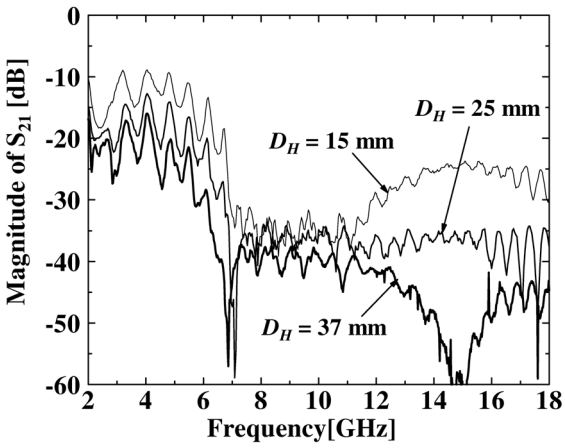

Figure 5: Magnitude of mutual coupling between two element APFA.

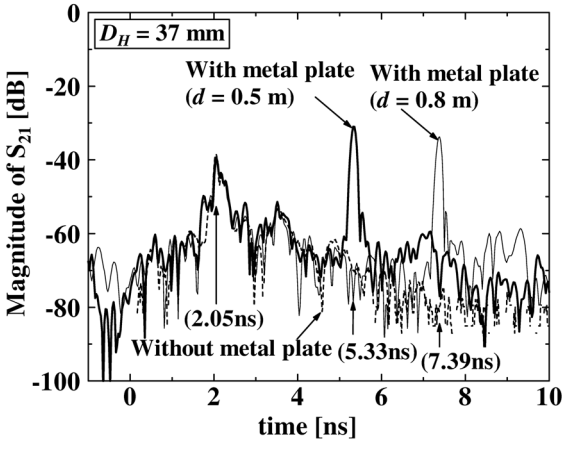

Figure 6: Pulse response for metal plate object.

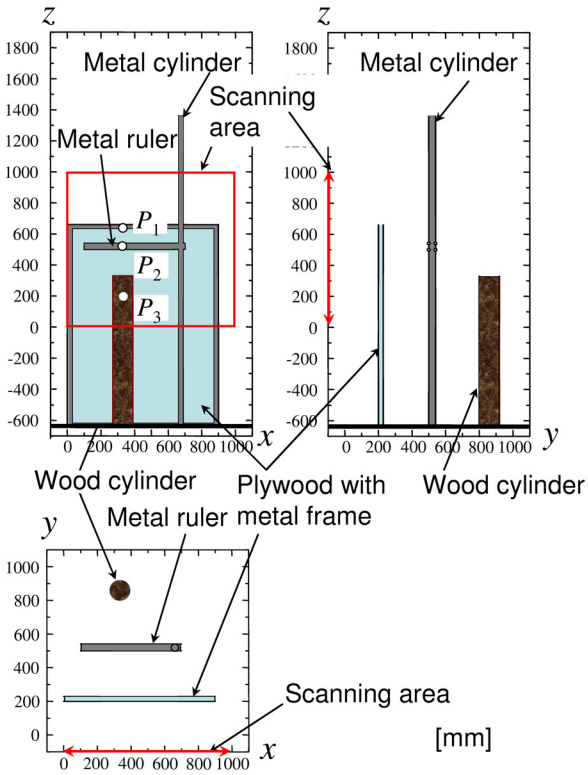

Figure 7: Experimental setup.

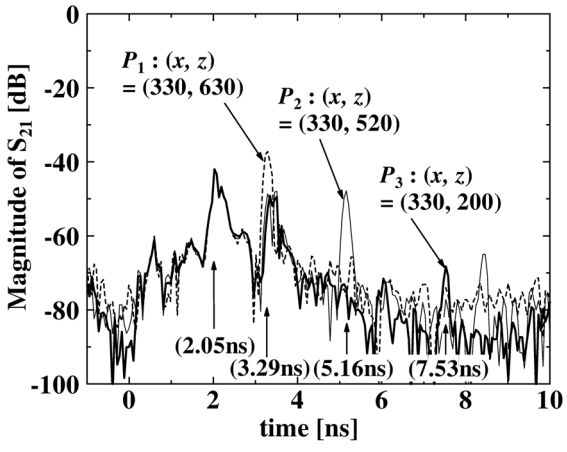

Figure 8: Pulse response at P_1, P_2 and P_3.

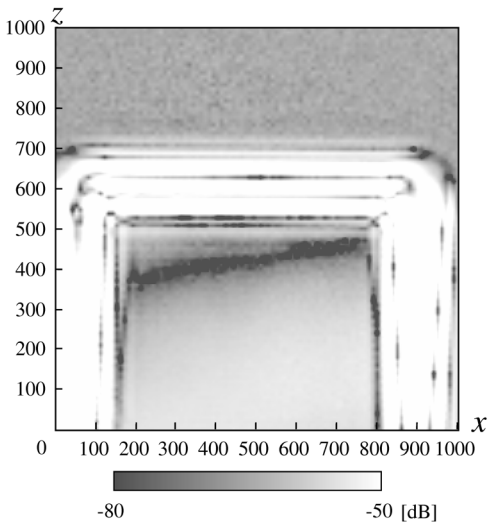

(a) t=3.29 ns

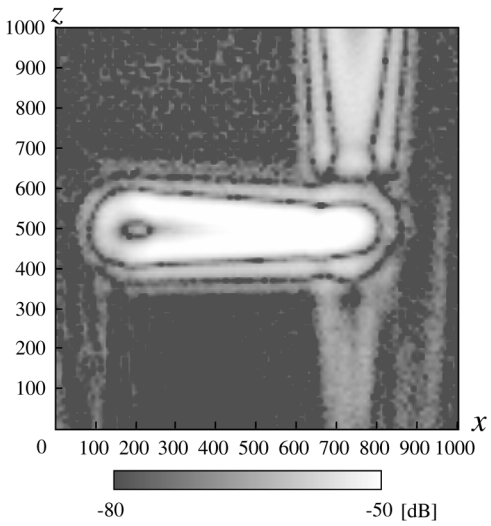

(b) t=5.16 ns

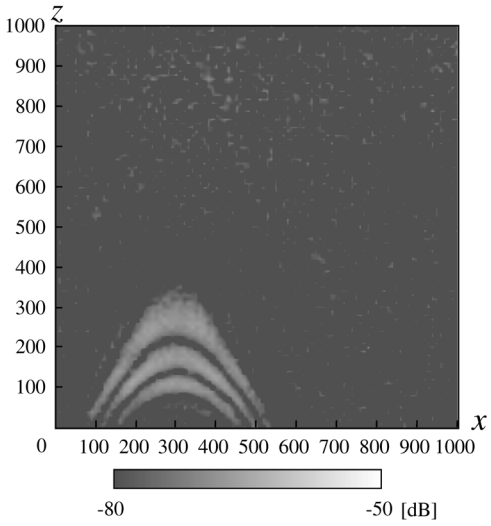

(c) t=7.53 ns

Figure 9: Magnitude of pulse response at t=3.29 ns, 5.16 ns and 7.53 ns in scanning area.